

# Androgen Receptor Is Targeted to Distinct Subcellular Compartments in Response to Different Therapeutic Antiandrogens

Hayley C. Whitaker,<sup>1</sup> Sarah Hanrahan,<sup>3</sup>  
Nick Totty,<sup>3</sup> Simon C. Gamble,<sup>1</sup>  
Jonathan Waxman,<sup>1</sup> Andrew C. B. Cato,<sup>4</sup>  
Helen C. Hurst,<sup>2</sup> and Charlotte L. Bevan<sup>1</sup>

<sup>1</sup>Prostate Cancer Research Group and <sup>2</sup>Cancer Research UK Molecular Oncology Unit, Department of Cancer Medicine, Faculty of Medicine, Imperial College London, London, United Kingdom;

<sup>3</sup>Protein Analysis, Cancer Research UK, London Research Institute, London, United Kingdom; and <sup>4</sup>Forschungszentrum Karlsruhe, Institute of Toxicology and Genetics, Karlsruhe, Germany

## ABSTRACT

**Purpose:** Antiandrogens are routinely used in the treatment of prostate cancer. Although they are known to prevent activation of the androgen receptor (AR), little is known about the mechanisms involved. This report represents the first study of the localization of wild-type AR following expression at physiologic relevant levels in prostate cells and treatment with androgen and antiandrogens.

**Experimental Design:** We have characterized a cellular model for prostate cancer using *in situ* cellular fractionation, proteomics, and confocal microscopy and investigated the effect of antiandrogens in clinical use on the subcellular localization of the AR.

**Results:** Different antiandrogens have diverse effects on the subcellular localization of the AR. Treatment with androgen results in translocation from the cytoplasm to the nucleoplasm, whereas the antiandrogens hydroxyflutamide and bicalutamide lead to reversible association with the nuclear matrix. In contrast, treatment with the antiandrogen cyproterone acetate results in AR association with cytoplasmic membranes and irreversible retention within the cytoplasm. In addition, we demonstrate that AR translocation requires ATP and the cytoskeleton, regardless of ligand.

**Conclusions:** These results reveal that not all antiandrogens work via the same mechanism and suggest that an

informed sequential treatment regime may benefit prostate cancer patients. The observed subnuclear and subcytoplasmic associations of the AR suggest new areas of study to investigate the role of the AR in the response and resistance of prostate cancer to antiandrogen therapy.

## INTRODUCTION

Prostate cancer is the most commonly diagnosed male cancer in the United States and the second leading cause of male cancer death (1). Prostate growth is initially androgen dependent; thus, treatment involves reducing circulating androgen levels using leuteinizing hormone-releasing hormone analogs and opposing androgen action using antiandrogens. Little is known about how antiandrogens elicit their effects, although they act at the level of the androgen receptor (AR), which mediates the effects of all androgens including the major circulating androgen testosterone and the more potent dihydrotestosterone (DHT).

The AR is a ligand-dependent transcription factor, closely related to the other steroid receptors, whose cellular localization patterns are diverse. Unliganded progesterone receptor is mainly cytoplasmic, whereas unliganded estrogen receptor is predominantly nuclear, but both shuttle between the cytoplasm and nucleus (2, 3). Conversely, unliganded glucocorticoid receptor resides entirely in the cytoplasm (4). There is controversy concerning the localization of unliganded AR: different groups have reported predominantly cytoplasmic or nuclear localization (5–9). The current consensus is that unliganded AR resides largely in the cytoplasm, complexed with heat shock proteins (10). On binding androgen, the AR is believed to dissociate from heat shock proteins, dimerize, translocate into the nucleus, and bind to androgen response elements, from which it promotes the transcription of androgen-regulated genes.

Antiandrogens bind to the AR but do not promote androgen-dependent gene transcription. It is unclear which steps in the AR signaling pathway are blocked by antiandrogens, and it was long thought that they simply competed with the ligand for binding to the AR or prevented nuclear import of the receptor. Although these factors may contribute to the overall effect of the drugs, they do not account for all their actions. In some systems antiandrogens have been shown to promote AR nuclear import and even DNA binding while still inhibiting androgen-responsive gene transcription (5, 6, 11, 12). Using reporter assays, several groups have shown partial AR activation in the presence of the therapeutic antiandrogens hydroxyflutamide (OHF) and cyproterone acetate (CPA), thus these are termed partial antagonists. Bicalutamide (BIC), beginning to be widely used in prostate cancer therapy, is thought to be a pure antagonist because no transactivation has yet been reported in its presence.

It is necessary to study how antiandrogens exert their effects to understand why hormone therapy for prostate cancer, while initially successful, inevitably fails. Investigations into the

Received 2/27/04; revised 7/27/04; accepted 8/11/04.

**Grant support:** The Prostate Cancer Charity and Cancer Research United Kingdom.

The costs of publication of this article were defrayed in part by the payment of page charges. This article must therefore be hereby marked *advertisement* in accordance with 18 U.S.C. Section 1734 solely to indicate this fact.

**Requests for reprints:** Charlotte L. Bevan, Prostate Cancer Research Group, Department of Cancer Medicine, Faculty of Medicine, Imperial College London, Du Cane Road, London W12 ONN, United Kingdom. Phone: 44-208-3833784; Fax: 44-208-3835830; E-mail: charlotte.bevan@imperial.ac.uk.

©2004 American Association for Cancer Research.

mechanism of action of antiandrogens in prostate cancer have been hampered by a lack of relevant cellular models for the disease. Previous studies have used transient overexpression of the AR (frequently tagged with other moieties, such as green fluorescent protein) or the LNCaP cell line, which has a mutated AR that affects translocation in the presence of antiandrogens (13). Here, we use a PC3 prostate cancer cell line that has been stably transfected with wild-type AR (PC3wtAR) to express homogenous levels of AR protein similar to the endogenous levels in target cells (14). Using a cell fractionation procedure, we have separated PC3wtAR cells into subcellular compartments including the cytoplasm, nucleus, and nuclear matrix (NM) and demonstrate for the first time alternative subnuclear and subcytoplasmic compartmentalization of wild-type AR after treatment with androgens and antiandrogens in a prostate cancer cell line.

## MATERIALS AND METHODS

**Cell Culture.** PC3wtAR (14) and LNCaP cells (American Type Culture Collection, Manassas, VA) were cultured in RPMI 1640 (Sigma, St. Louis, MO) supplemented with 100 units/mL penicillin, 0.1 mg/mL streptomycin, 2 mmol/L glutamine (Sigma), and 10% fetal bovine serum (Labtech International, Sussex, United Kingdom). PC3wtAR medium was supplemented with 4  $\mu$ g/mL Geneticin (Life Technologies, Inc., Rockville, MD). COS-1 cells were cultured in DMEM medium (Sigma) supplemented with penicillin, streptomycin, glutamine and serum as above. Culture in androgen-free conditions was carried out in "starvation media": phenol red-free RPMI or DMEM (Invitrogen, Carlsbad, CA) supplemented as above but with charcoal-stripped fetal bovine serum (Globepharm Surrey, United Kingdom).

Before *in situ* cell fractionation, PC3wtAR and LNCaP cells were grown to 60% confluence, washed three times in PBS (Sigma), and cultured in starvation medium for 24 hours. Cells were dosed with  $10^{-8}$  mol/L of the DHT analog mibolerone (MB; Perkin-Elmer, Fremont, CA) or  $10^{-6}$  mol/L antiandrogens [CPA (Sigma), OHF (Schering-Plough Hertfordshire, United Kingdom), or BIC (AstraZeneca, Cheshire, United Kingdom)] for 2 hours. For reversibility experiments, cells were grown and treated with antiandrogens and then washed three times in PBS, and fresh starvation medium was added, containing either  $10^{-8}$  mol/L MB or an equal volume of vehicle (EtOH), for 4 hours. For studies inhibiting the cytoskeleton and ATP hydrolysis, cells were treated with either 1 nmol/L cytochalasin D (Sigma) or 100 ng/mL nocodazole (Sigma) for 15 minutes or with 1 nmol/L oligomycin (Sigma) for 1 hour before treatment with ligand for an additional 2 hours. These treatments retained cell viability.

**Transfection of COS and PC3wtAR Cells.** Cells were grown in 24-well plates to 40% confluence, washed three times in PBS, and incubated in starvation medium for 24 hours. COS cells were transfected with 50 ng of pSG5-AR per well using FuGENE 6 (Roche, Mannheim, Germany) according to the manufacturer's instructions. Transfection efficiency was estimated after 48 hours by immunofluorescent labeling of the AR. PC3wtAR cells were transfected with 125 ng of mouse mammary tumor virus-LUC reporter (15) per well using FuGENE 6, grown for an additional 12 hours, and then treated for 48 hours

with either  $10^{-8}$  mol/L MB or  $10^{-6}$  mol/L antiandrogen. Luciferase activity was measured using the LucLite luciferase assay kit (Packard Bioscience, San Diego, CA). Each treatment was assayed in quadruplicate, and data are shown  $\pm$  SD.

***In situ* Cell Fractionation.** *In situ* cell fractionation was carried out immediately after incubation with ligand using a method modified from Staufienbiel and Deppert (16). Briefly, cells were incubated with the following buffers, and each was retained for immunoblotting: (a) wash buffer, 10 mmol/L MES (pH 6.3), 10 mmol/L NaCl<sub>2</sub>, 1.5 mmol/L MgCl<sub>2</sub>, 10% glycerol, and 5  $\mu$ L/mL mammalian protease inhibitor mixture (Sigma); (b) cytoplasmic buffer, wash buffer plus 1% Nonidet P-40, 1 mmol/L EGTA, 5 mmol/L dithiothreitol (DTT) for 3 (C1) and 27 (C2) minutes sequentially at 4°C; (c) DNase I buffer, wash buffer plus 50  $\mu$ g/mL DNase I for 15 minutes at 37°C; (d) nuclear buffer, 4 mol/L NaCl<sub>2</sub>, 10 mmol/L MES (pH 6.2), 1.5 mmol/L MgCl<sub>2</sub>, 10% glycerol, and 5  $\mu$ L/mL mammalian protease inhibitor mixture, 1 mmol/L EGTA, and 5 mmol/L DTT for 30 minutes at 4°C; (e) RNase A buffer, wash buffer plus 50  $\mu$ g/mL DNase I and 50  $\mu$ g/mL RNase A for 30 minutes at 37°C; (f) NM buffer, 50 mmol/L Tris (pH 9), KCl, 3% (v/v) Empigen BB (Ellis & Everard Yorkshire, United Kingdom), 5 mmol/L DTT, 1 mmol/L EGTA, 10% glycerol, and 5  $\mu$ L/mL mammalian protease inhibitor mixture for 1 hour at 4°C; and (g) urea buffer, 9 mol/L urea, 2% (w/v) CHAPS, 1% (w/v) DTT, 2% (v/v) pharmalytes (Amersham Biosciences, Piscataway, NJ) for 5 minutes at room temperature with scraping.

**Immunoblot Analysis.** Cell pellets were solubilized in urea buffer to give whole cell lysates. For these and cellular fractions, protein concentration was determined using Bradford reagent (Bio-Rad, Hercules, CA), and equal amounts of total protein were loaded. Samples were separated by SDS-PAGE and transferred onto nitrocellulose membrane (Bio-Rad) before probing for AR using either PG-21 antibody (Upstate Biotechnology, Lake Placid, NY) or AR441 (Dako Cytomation, Copenhagen, Denmark). Control blots were probed with anti-actin (Sigma), anti-Hsp60 (Stressgen, San Diego, CA), anti-poly-(ADP-ribose) polymerase (PARP; Santa Cruz Biotechnology, Santa Cruz, CA), or anti-lamin B (Santa Cruz Biotechnology). Blots were incubated with the appropriate horseradish peroxidase-conjugated secondary antibody (Dako Cytomation) diluted 1:1,000 and visualized using ECL-Plus (Amersham Biosciences).

**Immunofluorescence.** Cells were grown on sterile glass coverslips in 24-well plates to 30% confluence in RPMI 1640 and washed three times in PBS, and starvation medium was added for 24 hours. They were then dosed with either  $10^{-8}$  mol/L MB or  $10^{-6}$  mol/L antiandrogen for 2 hours, washed three times in PBS, and fixed in methanol at  $-20^{\circ}\text{C}$  for 10 minutes. Before probing with a primary antimouse or antirabbit antibody, cells were treated with 10% whole goat serum (Dako) in PBS for 30 minutes; for primary antigoaat antibodies, 10% whole rabbit serum (Dako) was used. Mouse anti-Hsp60, anti-PARP, and anti-actin antibodies and rabbit anti-transferrin (Abcam, Cambridge, United Kingdom), anti-albumin (Sigma), anti-Hsp90 (Santa Cruz Biotechnology), and anti-manganese-binding superoxide dismutase (MnSOD) antibodies were applied (1:200) to the cells in 10% whole goat serum; goat anti-lamin B and anti-GRP 78 antibodies (Santa Cruz Biotech-

nology) were applied (1:200) in 10% whole rabbit serum, all for 1 hour. Cells were washed three times in PBS, and 10% whole goat or rabbit serum was applied for 15 minutes before incubation with a fluorescein isothiocyanate isomer I (FITC)- or tetramethylrhodamine isothiocyanate-conjugated secondary antibody (Sigma) for 1 hour. After five washes in PBS, coverslips were mounted on glass slides with Vectashield containing 4',6-diamidino-2-phenylindole (DAPI; Vector Laboratories, Burlingame, CA). Slides were visualized on a Zeiss Meta 512 confocal microscope, and an average of 16 images was captured. For reversibility experiments, PC3wtAR cells were grown and treated with antiandrogens and then MB or vehicle, as described previously, before fixing.

**Two-Dimensional Gel Electrophoresis.** After cell fractionation, each fraction was prepared for two-dimensional gel electrophoresis (2-DE). The nuclear fraction (N; 5 mL) was placed in a 10,000 Da Slide-A-lyzer (Pierce, Rockford, IL) and rotated in 1 liter of dialysis buffer [10 mmol/L MES (pH 6.2), 1.5 mmol/L MgCl<sub>2</sub>, 1 mmol/L EGTA, and 5 mmol/L DTT] for 24 hours at 4°C, with a change of buffer after 8 hours. The C1 (membrane-associated), C2 (cytoplasmic), N (nuclear), NM, and U (9 mol/L urea buffer) fractions were concentrated by adding high-performance liquid chromatography-grade acetone (Sigma) to give at least 80% acetone, inverting the samples several times and incubating them on ice for 30 minutes before collecting the protein pellet by centrifugation (15,000 rpm for 15 minutes). The pellet was air dried and solubilized in a small volume of thiourea lysis buffer [2 mol/L thiourea (Sigma), 7 mol/L urea, 2% (w/v) CHAPS, 1% (w/v) DTT, 4% (v/v) pharmalytes (Amersham Biosciences)]. Before 2D-E, 125 μL of concentrated sample was diluted with 125 μL of rehydration buffer [8 mol/L urea, 0.5% CHAPS, 0.2% DTT, and 0.2% pharmalyte (pH 3–10)]. The prepared protein samples were applied to 13-cm IPG strips [Amersham Biosciences; pH range, 3–10 (non-linear)] during gel rehydration according to the manufacturer's instructions. Proteins were focused at 350 V for 105 minutes, an increasing gradient from 350 to 3,500 V for 105 minutes, followed by 3,500 V for 17 h. Then, strips were equilibrated in equilibration buffer [1.5 mol/L Tris (pH 8.8) buffer containing 6 mol/L urea, 30% glycerol, 2% SDS, and 0.01% bromphenol blue] with the addition of 1% DTT for 15 minutes. Buffer was replaced by equilibration buffer supplemented with 4.8% iodoacetamide for 15 minutes. Proteins were separated on 12% SDS-PAGE gels, and the gels were fixed in 50% methanol, 10% acetic acid for 2 hours and placed in SYPRO-ruby stain (Bio-Rad) overnight at 4°C. After washing in water for 30 minutes, gels were visualized on a Typhoon 8600 variable mode imager (Amersham Biosciences).

**Protein Identification by Mass Spectrometry.** Protein spots from each gel were excised using a sterile pipette tip, washed with water and then with 25 mmol/L ammonium bicarbonate and acetonitrile (Rathburn Chemicals, Walkerburn, United Kingdom), and dehydrated for 10 minutes in a speed vac. They were then washed with 25 mm ammonium bicarbonate and acetonitrile again before dehydration. After a 4-hour digestion with trypsin (50 ng; Promega, Madison, WI) in 25 mmol/L ammonium bicarbonate, the peptides were extracted using two washes of 5% formic acid in water. Each extraction was sonicated for 10 minutes, and the pooled extracts were dried down

in siliconized tubes. Peptides were then resuspended in 20 μL of water, vacuum dried, washed with water, and finally dried completely to remove volatile salts.

Peptide extracts were used for matrix-assisted laser desorption ionization time-of-flight (TOF) or nano-lc quadrupole-TOF mass spectrometric analysis. matrix-assisted laser desorption ionization TOF/TOF mass spectra were recorded with an Applied Biosystems (Foster City, CA) 4700 using α-cyano-4-hydroxycinnamic acid [Sigma; 10 μg/μl in 50% (v/v) acetonitrile and 0.1% (v/v) trifluoroacetic acid (Pierce)] as a matrix. Spectra were internally calibrated by the inclusion of 20 fmols of angiotensin I (Sigma) or a trypsin autolysis peptide. The peptide masses were searched against the National Center for Biotechnology Information nonredundant database using the Protein Prospector MS-FIT<sup>5</sup> or Mascot<sup>6</sup> programs. One missed cleavage per peptide and an initial mass tolerance of 10 ppm were used in all searches.

Electrospray mass spectra were recorded using a quadrupole-TOF mass spectrometer (Micromass) interfaced to a Dionex nano-lc system. Samples were dissolved in 0.1% formic acid, injected onto a 75 μm × 150-mm pepmap column (Dionex), and eluted with an acetonitrile/0.1% formic acid gradient at 200 nl/min. Capillary voltage was set to 3750 V, and data dependent tandem mass spectrometry acquisitions were performed on multiply charged precursors. Proteins were identified by searching National Center for Biotechnology Information database using Protein Prospector MS-TAG or MS-PATTERN programs. Initial mass tolerance was 50 ppm for precursors and 150 ppm for fragment ions.

## RESULTS

**PC3wtAR Cells Are a Relevant Model for Prostate Cancer.** We examined the level of AR expressed in PC3wtAR cells as compared with endogenous AR expression in the LNCaP prostate cell line (13), the T47D breast cancer cell line (17), and COS cells transiently transfected with wtAR (Fig. 1A). The expression level of AR in PC3wtAR cells was greater than that in T47D cells and comparable with that in LNCaP cells. As expected, the parental PC3 cells expressed no AR. In this experiment, only 25% of the COS cells were transfected (data not shown), yet levels of AR were comparable with those in LNCaP cells, demonstrating hyperphysiological AR expression in the transfected fraction. Furthermore, immunofluorescent staining showed wide variation in expression levels between the transfected COS cells, whereas PC3wtAR and LNCaP cells were homogenous for AR expression (data not shown). Finally, we confirmed that the AR in PC3wtAR can activate transcription of an androgen-responsive reporter gene in a ligand-dependent manner, demonstrating that the AR is functional in these cells (Fig. 1B; ref. 14). In support of this, we have previously demonstrated that the AR in these cells is capable of down-regulating endogenous prohibitin protein in response to androgen stimulation, to a similar extent as seen in the LNCaP cell line (18).

<sup>5</sup> www.prospector.ucsf.edu/.

<sup>6</sup> www.matrixscience.com.



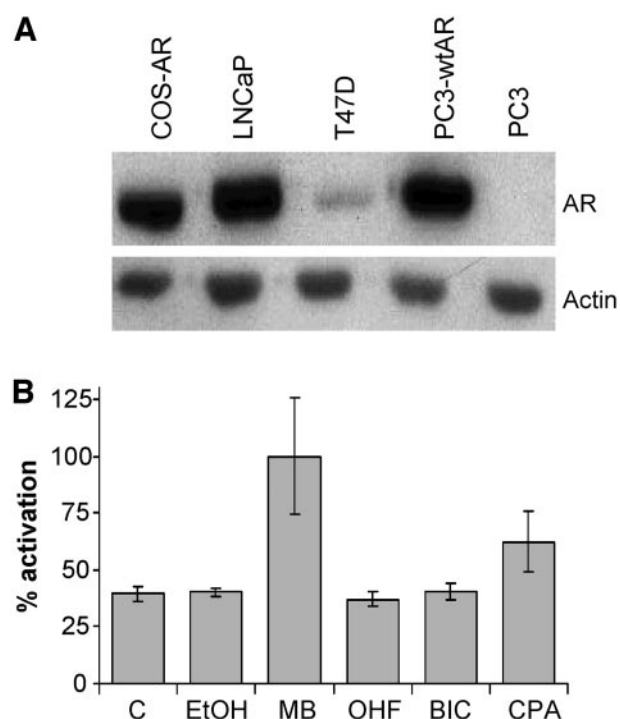


**Fig. 1** PC3wtAR cells express physiologic levels of functional AR. **A**. Whole cell lysates (20  $\mu$ g) immunoblotted with anti-AR antibody revealed a specific band at 110 kDa. Blots were reprobed for actin (loading control; *bottom panel*). **B**. PC3wtAR cells were transiently transfected with an androgen-responsive luciferase reporter. Luciferase activity in the presence of vehicle or antiandrogens ( $10^{-6}$  mol/L) is expressed as a percentage of activity in the presence of ligand (MB,  $10^{-8}$  mol/L). **C**, control lacking androgen response element; *EtOH*, vehicle control.

### ***In situ* Cell Fractionation Effectively and Efficiently Separates Cellular Compartments of PC3wtAR Cells.**

To study the effects of antiandrogens on AR translocation, a sequential *in situ* cell fractionation procedure was developed. Effective fractionation of the cells was demonstrated by immunoblotting using antibodies to known markers for the cytoplasm, nucleus, and NM (Fig. 2A). Results were confirmed using immunofluorescent microscopy on intact cells (Fig. 2B). Hsp60, a cytoplasmic and mitochondrial protein (19), was found only in the cytoplasmic fractions (C1 and C2), and confocal microscopy confirmed the absence of any nuclear staining. The nuclear marker PARP (20) was only visible in the nuclear fraction (N) of cells by immunoblotting and was seen to be exclusively nuclear using immunofluorescence. Thus we found no contamination between the cytoplasmic and nuclear fractions. Separation of the NM fraction was confirmed using an anti-lamin B antibody (21). Some lamin B was also found in the residual 9 mol/L urea buffer fraction (U), demonstrating incomplete solubilization of NM proteins in the NM fraction. Immunofluorescence confirmed lamin B staining in the nuclear lamina and nuclear speckles of PC3wtAR cells. The *in situ* cell fractionation method is reported to be exhaustive for each fraction while retaining the cellular architecture (16). By confocal microscopy, we were able to confirm the complete removal of our markers

(Hsp60, PARP, and lamin B) after the relevant fractionation step, confirming that each buffer removes the appropriate fraction from the cells while leaving subsequent fractions intact (data not shown).

### **Characterization of PC3wtAR Subcellular Fractions.**

To place the AR in a defined context within each subcellular fraction, the protein-rich fractions (C1, C2, N, NM, and U) were separated by 2-DE, and major protein features were selected for

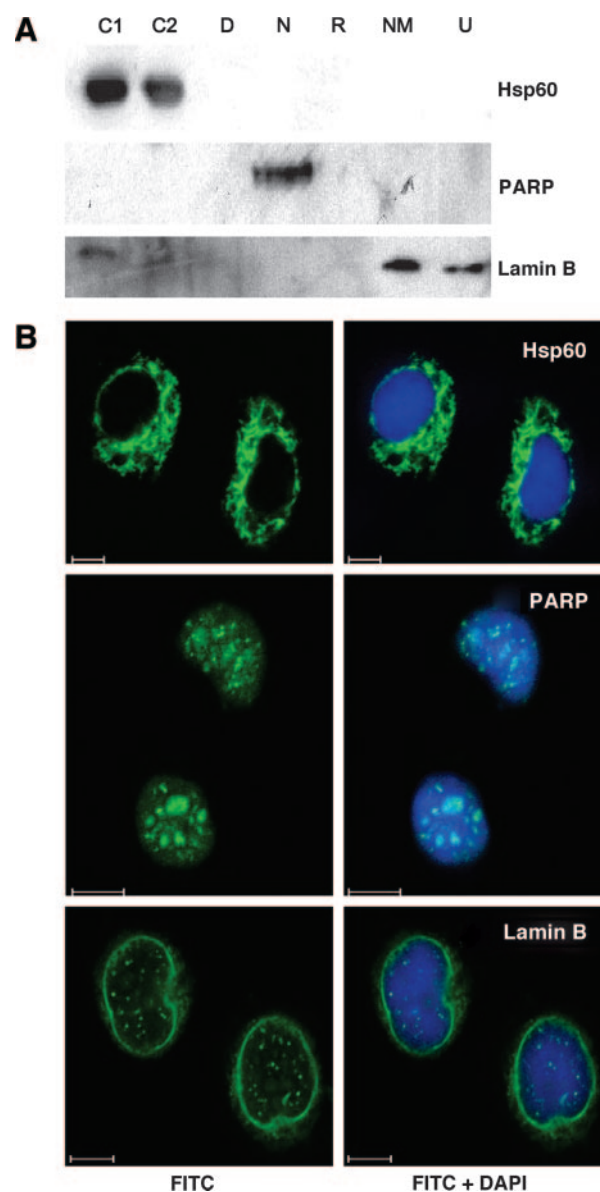


**Fig. 2** *In situ* cell fractionation effectively separates cellular components of PC3wtAR cells. **A**. Thirty micrograms of protein from each fraction of PC3wtAR cells were immunoblotted for Hsp60, PARP, or lamin B as indicated. Fractions: **C1**, membrane-associated; **C2**, cytoplasmic; **D**, DNase I treated; **N**, nuclear; **R**, RNase A/DNase I treated; **U**, 9 mol/L urea buffer. **B**. The same antibodies were used to probe intact cells, and proteins were visualized using FITC-labeled secondary antibody (green). The nucleus was visualized using DAPI (blue). Scale bars, 10  $\mu$ m.

Table 1 A selection of major features from each cell fraction 2-DE, identified by mass spectrometry

| Accession no. *                   | Name   | Subcellular location †                      |
|-----------------------------------|--|---|
| (C1) Membrane-associated proteins |  |   |
| 2501351                           | Serotransferrin precursor (22)   | Membrane associated                         |
| 113576                            | Serum albumin precursor (35)   | Cytoplasm, membrane associated and secreted |
| 1657237                           | Heat shock 70-kDa protein 5/BiP/GRP78 (26)                                 | Endoplasmic reticulum/cytoplasm             |
| 4501881/4501885                   | $\alpha$ - or $\beta$ -Actin (29)  | Structural protein                          |
| 30841309                          | Manganese-binding superoxide dismutase (Mn SOD) (34)                       | Mitochondria                                |
| 4502551                           | Calumenin (23)   | Secreted, endoplasmic reticulum             |
| (C2) Cytoplasmic proteins         |  |   |
| 113576                            | Serum albumin precursor (35)   | Cytoplasm, membrane associated and secreted |
| 1657237                           | Heat shock 70-kDa protein 5/BiP/GRP78 (26)                                 | Endoplasmic reticulum/cytoplasm             |
| 4505839                           | Pyruvate kinase (24)   | Cytoplasm                                   |
| 13129150                          | Heat shock 90-kDa protein 1 (10)   | Cytoplasm                                   |
| 5453603                           | Chaperonin-containing t-complex polypeptide-1 $\beta$ (25)                 | Cytoplasm                                   |
| (N) Nuclear proteins              |  |   |
| 4826998                           | Polypyrimidine tract binding protein-associated splicing factor (PSF) (27) | Nucleus                                     |
| 4885511                           | Nucleolin (28)   | Nucleus                                     |
| 2119276                           | $\beta$ -Tubulin (25)  | Structural protein                          |
| 4501881/4501885                   | $\alpha$ - or $\beta$ -Actin (29)  | Structural protein                          |
| (NM) Nuclear matrix proteins      |  |   |
| 27436946                          | Lamin A/C precursor (21)   | Nuclear matrix                              |
| 15809016/                         | Myosin regulatory light chain  | Structural protein                          |
| 5453740                           | MRCL2/MRCL3 (30)   |   |
| 4557888                           | Keratin 18 (31, 32)  | Structural protein                          |
| 24234699                          | Keratin 19 (31)  | Structural protein                          |
| (U) NM urea lysis buffer proteins |  |   |
| 27436946                          | Lamin A/C precursor (21)   | Nuclear matrix                              |
| 9624998                           | Heterogeneous nuclear ribonuclear protein H (33)                           | Nuclear matrix                              |
| 27436951                          | Lamin B2 (21)  | Nuclear matrix                              |
| 4507895                           | Vimentin (32)  | Intermediate filaments                      |
| 5031877                           | Lamin B1 (21)  | Nuclear matrix                              |
| 113576                            | Serum albumin precursor (35)   | Cytoplasm, membrane associated and secreted |

\* Accession number refers to the National Center for Biotechnology Information identification number.

† Information on subcellular localization was derived from previously published studies.

sequencing by mass spectrometry. After identification of proteins, the subcellular localization and basic function of each were determined from the current literature and are shown in Table 1. Many of the proteins appearing in C1, the membrane-associated fraction, were also found in the cytoplasmic fraction (C2). Similarly there was a high degree of crossover between the NM and 9 mol/L urea (U) fractions. These areas of overlap had already been suggested by the localization of Hsp60 and lamin B (Fig. 2). Known secreted proteins such as transferrin (22) and calumenin (23) were identified solely in C1. The cytoplasmic fraction C2 contained known cytoplasmic proteins such as pyruvate kinase (24), chaperonin-containing t-complex polypeptide-1 $\beta$  (25), and glucose-regulated protein 78 (GRP78; an endoplasmic reticulum chaperone protein; ref. 26). The nuclear fraction (N) contained polypyrimidine tract binding protein-associated splicing factor and nucleolin, proteins involved in transcriptional regulation and RNA maturation (27, 28), as well as structural proteins. The NM and U fractions contained proteins found in the cell cytoskeleton and intermediate filaments, such as actin (29), myosin (30), keratins (31, 32), and vimentin (32), as well as classical NM proteins such as lamins (21) and heterogeneous nuclear ribonucleoprotein H (33).

Immunofluorescent microscopy was used to confirm the localization of some of the identified proteins (Fig. 3). Actin, identified in the C1 and U fractions, can be seen at the

periphery of the cells as well as throughout the cell. Transferrin was identified in the membrane-associated cytoplasmic C1 fraction and can be seen both in the cytoplasm and associated with the cell membrane. GRP78 was present in the membrane-associated and cytoplasmic fractions. Confocal microscopy supports this, although some GRP78 can also be seen in nuclear speckles. hSP90 was confirmed in the cytoplasm and excluded from vacuoles, and small amounts could also be seen in the nucleus. MnSOD (34) was sequenced from the membrane-associated fraction, although confocal microscopy places the majority in the mitochondria. Immunoblotting confirmed that MnSOD is present in the C2 fraction as well as the C1 fraction but was not selected for sequencing (data not shown). Albumin (35) was found throughout the cytoplasm, with stronger staining detected at the cell periphery, supporting its identification in the C1 and C2 fractions. Large nuclear albumin speckles were also seen, in agreement with its presence in the 9 mol/L urea (U) fraction.

**Androgens and Antiandrogens Can Target Androgen Receptor to Different Subcellular Compartments.** The localization of AR in response to ligands was investigated. Cells were treated with the DHT analog MB or vehicle for 2 hours and then subjected to cell fractionation and immunoblotting for AR (Fig. 4, *top panel*). These results were supported by immunofluorescence studies (Fig. 4, *bottom panel*). In cells treated with

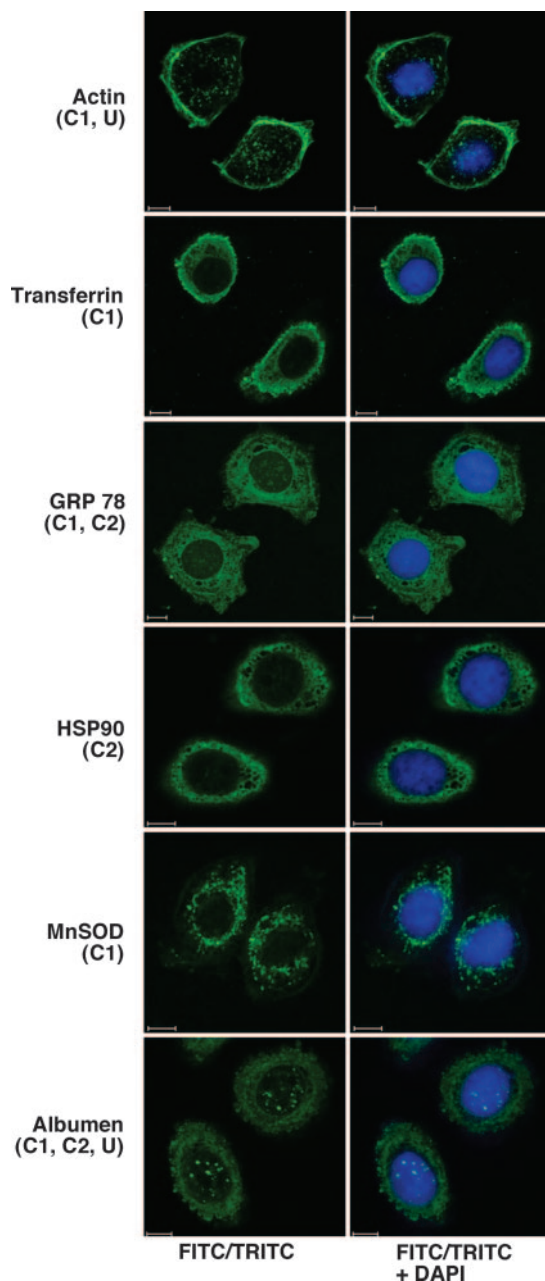


**Fig. 3** Cellular localization of a selection of proteins identified by 2-DE. PC3wtAR cells were grown to 30% confluence and fixed before probing with antibodies to actin, transferrin, GRP78, Hsp90, MnSOD, and albumin at a dilution of 1:200. Goat antimouse FITC-labeled antibody or rabbit anti-goat tetramethylrhodamine isothiocyanate-labeled antibody was used to visualize the proteins (green). The nucleus was visualized using DAPI (blue). Scale bars, 10  $\mu$ m.

vehicle, unliganded AR was found predominantly in the cytoplasm with a small amount present in the nucleus (Fig. 4A). This may be unliganded nuclear AR, or low levels of residual androgens in the media may result in some AR targeting to the nucleus. Conversely, in cells treated with MB, the liganded AR was found predominantly in the nucleus (Fig. 4B).

We next examined AR targeting by antiandrogens in PC3wtAR cells treated with  $10^{-6}$  mol/L antiandrogens for 2 hours (Fig. 4C–E). In cells treated with OHF or BIC, the AR localized largely to the NM and cytoplasmic fractions (Fig. 4C and D). After treatment with CPA, some nuclear localization of AR was seen, although the majority was retained in the cytoplasmic and membrane-associated fractions (Fig. 4E). These results were supported by immunofluorescence studies (Fig. 4, C–E, bottom panel), in which FITC-labeled AR was diffuse in the cytoplasm of cells treated with BIC and OHF but could also be seen in a distinct ring surrounding the nucleus (Fig. 4C) or in nuclear speckles (Fig. 4D), and CPA-treated cells showed the majority of fluorescence in the cytoplasm (Fig. 4E).

**Androgen Receptor Translocation after Treatment with Antiandrogens Can Be Reversible.** To determine whether AR binding to the NM and membrane-associated cytoplasmic fraction is reversible, PC3wtAR cells were treated first with antiandrogen for 2 hours and then washed before adding either MB or vehicle for an additional 4 hours before cell fractionation or immunofluorescence. Treatment of cells first with OHF or BIC, followed by vehicle or MB, revealed that the AR was able to relocate to either predominantly the cytoplasm (Fig. 4C and D, *i* compared with A) or the nucleus (Fig. 4C and D, *ii* compared with B), respectively, demonstrating that antiandrogen-induced binding of AR to the NM is reversible. When cells were treated with CPA followed by vehicle, the majority of AR moved from the C1, C2, and N fractions to the cytoplasmic C2 fraction, similar to results seen with treatment with vehicle alone (Fig. 4E, *i* compared with B). However, when cells were treated with MB after CPA treatment, some of the AR was able to relocate to the nucleus, but a large proportion of it remained in the cytoplasm (Fig. 4E, *ii*), demonstrating that AR translocation after treatment with CPA is only partially reversible.

**Androgen Receptor Translocation Requires ATP and the Cytoskeleton.** To assess whether AR translocation in response to antiandrogens is an active process, PC3wtAR cells were treated with the ATPase inhibitor oligomycin before hormone treatment and fractionation (Fig. 5A). The AR was found in the cytoplasm after treatment with vehicle, androgen, or antiandrogens, suggesting that ATPase activity is essential for all AR translocation. When actin polymerization was inhibited using cytochalasin D (Fig. 5B), the AR was unable to translocate to the nucleus after treatment with androgen, in agreement with previous work by Ozanne *et al.* (36). Antiandrogens were also unable to promote AR translocation after cytochalasin D treatment. Inhibition of tubulin polymerization using nocodazole (Fig. 5C) permitted limited AR translocation: in cells treated with MB, CPA, and OHF, AR was found in the NM as well as in the cytoplasmic fraction. However, in BIC-treated cells, AR remained completely cytoplasmic.

## DISCUSSION

The vast majority of prostate tumors (primary and metastatic) retain AR expression, so a cell line expressing wild-type AR would be most representative of the disease. However, prostate tumor cells generally lose expression of the AR gene after a few days in culture. The only widely available, immortal, AR-positive prostate cancer cell line, LNCaP, has a threonine to



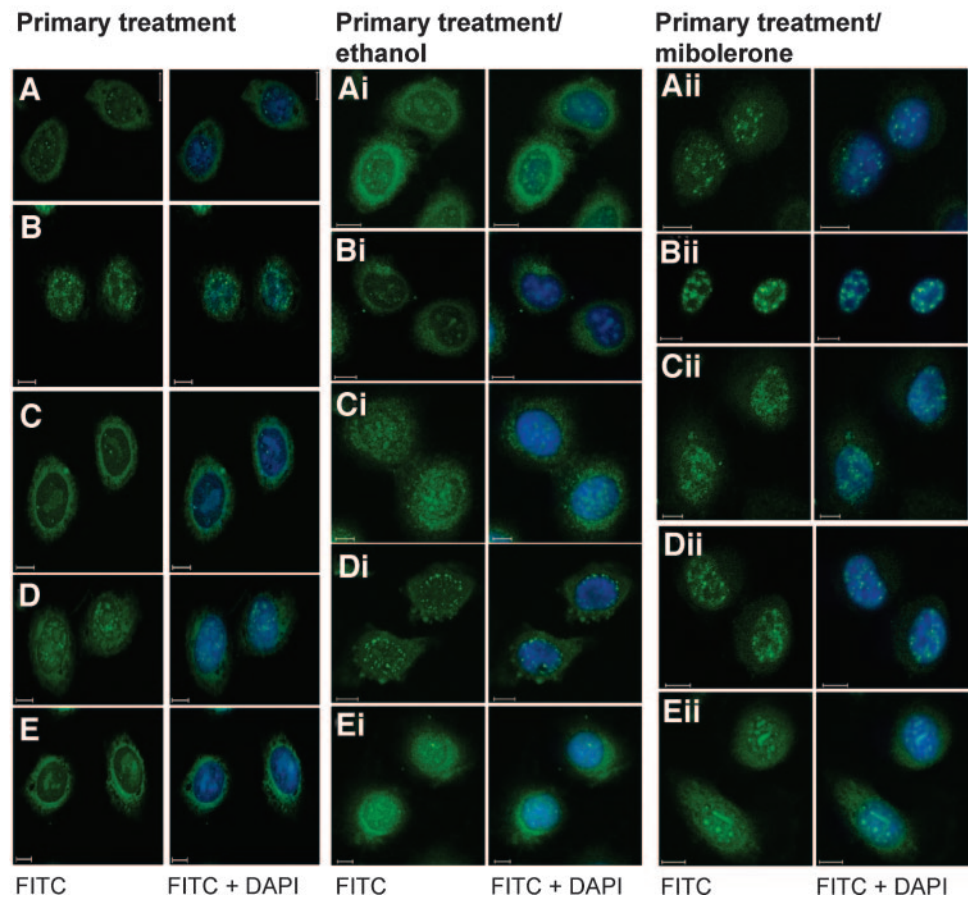
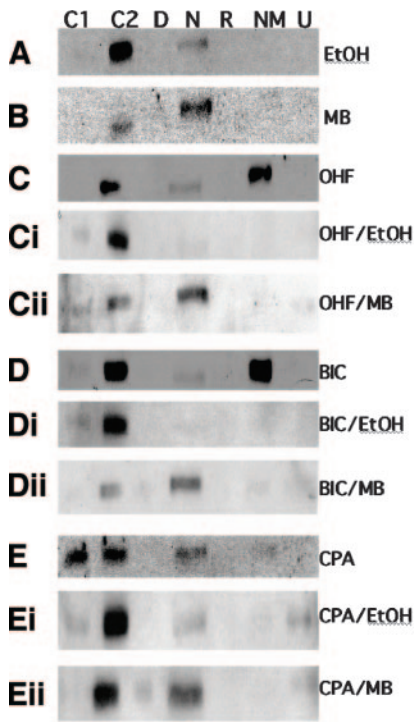


*Fig. 4* Androgen receptor targeting in PC3wtAR cells. PC3wtAR cells were treated with vehicle (A),  $10^{-8}$  mol/L MB (B), or  $10^{-6}$  mol/L OHF (C), BIC (D) or CPA (E) for 2 hours. Then, analysis was carried out as described below, or cells were first washed and treated with vehicle (i) or  $10^{-8}$  mol/L MB (ii) for an additional 4 hours. *Top panel.* *In situ* cell fractionation was carried out, and 30  $\mu$ g of protein from each fraction were immunoblotted for AR. *Bottom panel.* Cells grown on coverslips and treated as described above were fixed and probed with anti-AR antibody and visualized with FITC-labeled secondary antibody (green). The nucleus was visualized using DAPI (blue). *Scale bars,* 10  $\mu$ m. Fractions: C1, membrane associated; C2, cytoplasmic; D, DNase I treated; N, nuclear; R, RNase A/DNase I treated; and U, 9 mol/L urea buffer.

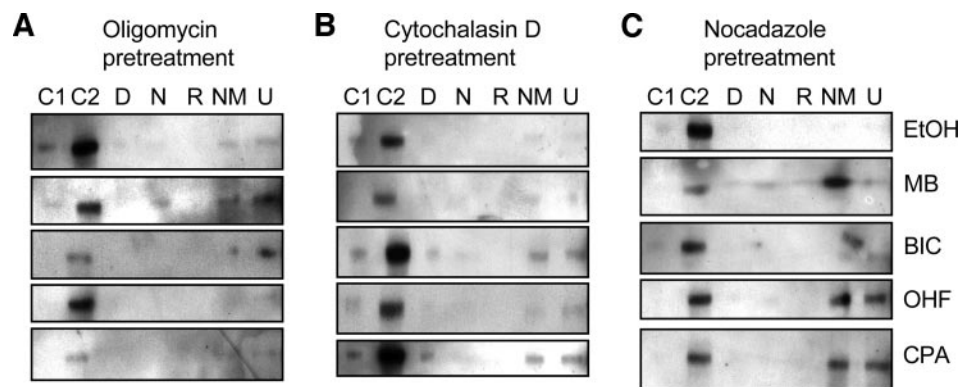


**Fig. 5** Androgen receptor translocation requires ATP and the cytoskeleton. PC3wtAR cells were treated with 1 nmol/L oligomycin for 1 hour (A), 1 nmol/L cytochalasin D for 15 minutes (B), or 100 ng/mL nocodazole for 15 minutes (C) before treatment with vehicle, ligand, or antiandrogens for 2 hours. Cells were fractionated *in situ*, and 15  $\mu$ g of protein from each fraction were immunoblotted for AR. Fractions: C1, membrane associated; C2, cytoplasmic; D, DNase I treated; N, nuclear; R, RNase A/DNase I treated; and U, 9 mol/L urea buffer.

alanine substitution at AR residue 877 (T877A; ref. 13). Whereas this mutant receptor remains responsive to androgens, it is also activated by estradiol and several antiandrogens, and the mutation appears to affect nuclear translocation of the receptor (8, 13), hence LNCaP cells are not optimal for studying antiandrogen action. An alternative is to use AR-negative cell lines transiently transfected with wild-type AR. However, this introduces possible artifacts due to overexpression and wide variation in levels within the transfected cell population. Previously, the speed and degree of ligand-dependent AR translocation have been shown to be highly dependent on cell type and AR expression level, with different groups reporting either complete or incomplete translocation (5–9). Here we are using PC3 cells, an AR-negative prostate cancer cell line, which has been stably transfected with wild-type AR. These cells homogeneously express levels of AR comparable with LNCaP cells, and the receptor translocates from the cytoplasm to the nucleus on addition of ligand. Reporter assays demonstrated that the AR is functional, and furthermore, it is able to mediate down-regulation of an endogenous target protein (18). We believe therefore that these cells represent a relevant model in which to study AR activity in androgen-sensitive prostate cancer.

To determine categorically the cellular compartment to which AR translocates in response to different treatments, we modified a protocol to fractionate the cells into two cytoplasmic fractions (the first containing the majority of membrane-associated proteins), a nuclear fraction and a NM fraction (16). This enabled us not only to determine the subcellular localization but also, for the first time, to localize the AR into subcytoplasmic and subnuclear fractions. In cells treated with the nonsteroidal antiandrogens BIC and OHF, roughly equal amounts of AR protein were found in the NM fraction and the cytoplasm, with a relatively very small amount in the nucleoplasmic fraction. Conversely, the steroidal antiandrogen CPA did not target AR to the NM. In CPA-treated cells, the bulk of AR was found equally divided between the two cytoplasmic fractions, with a small amount in the nuclear fraction. Previous studies using transiently transfected COS and prostate cells reported antiandrogens targeting AR to the nucleus (5–9), whereas we see only a

small fraction of AR in the salt-soluble nuclear fraction. We believe this is partly because our method separates nuclear and NM proteins, which were previously treated as a single cellular compartment. We show that all antiandrogens tested retain AR in the cytoplasm of PC3wtAR cells to varying degrees. The retention appears to be greater than that in transiently transfected cells (6, 7, 9). We propose that this partial cytoplasmic retention may be a more accurate reflection of the movement of endogenous AR and that complete nuclear translocation in the presence of antiandrogens in transfected cells could be an artifact of transient AR overexpression. However, cytoplasmic retention is not the only mechanism of action of these antiandrogens. The appearance of a substantial fraction of AR in the NM in the presence of OHF and BIC shows that another mechanism must also be occurring by which AR activity is inhibited by these compounds, which may involve a specific AR conformation or specific cofactors. Masiello *et al.* (12) demonstrated that even when BIC-occupied AR is bound to DNA, it is inactive, presumably due to alterations in cofactor recruitment. It is possible that the NM-associated AR may represent AR in such inactive complexes, whereas AR in the nuclear fraction is active. Alternatively, the small amount of AR seen in the nuclear fraction may represent the inactive DNA-bound fraction seen by Masiello *et al.* (12). Additional studies will determine whether there are differences in the proteins bound by AR between the nuclear and NM fractions.

In the presence of CPA, a larger proportion of total AR is nuclear, but because CPA has been shown to have partial agonist activity on wild-type AR, this may represent active receptor (13). In support of this, we carried out *in situ* cell fractionation of the LNCaP cell line and found that a relatively much greater proportion of AR is nuclear in these cells in the presence of OHF and CPA (approximately 30%).<sup>7</sup> This is unsurprising because both CPA and OHF are able to activate the AR T877A mutant found in LNCaP cells to almost the same

<sup>7</sup> H. Whitaker, S. Gamble, C. Bevan, Unpublished results.



degree as ligand (13). Hence, *in situ* cell fractionation can identify active AR in the nuclear fraction irrespective of whether this is wild-type AR activated by androgen binding or mutant AR aberrantly activated by alternative ligands. Whereas AR targeted to the NM by OHF and BIC was able to relocate to the nuclear fraction on subsequent treatment with ligand, the same was not true for the cytoplasmic CPA-bound AR. Although CPA has a higher relative binding affinity for AR than OHF and BIC, this is only in the order of 4-fold (13); hence, it is unlikely to explain the observed difference in reversibility. Furthermore, CPA is clearly able to dissociate from the receptor because the AR seen in the C1 and nuclear fractions in the presence of CPA efficiently moves into the cytoplasm (C2) after subsequent EtOH treatment, and it is only movement from the cytoplasm into the nucleus on androgen treatment that appears to be inhibited. The mechanism of this cytoplasmic retention is unclear, but this observation suggests that a major mechanism of CPA action may be preventing AR translocation to the nucleus.

Despite androgens and antiandrogens working via different mechanisms, it would appear that they all require ATPase activity and an active cytoskeleton. After ATPase inhibition, AR was unable to translocate from the cytoplasm to any other fraction. This may reflect loss of ligand binding because the ATPase activity of the heat shock protein complex is thought to be required for opening and maintaining an active ligand binding pocket (10). Alternatively, ATPase inhibition could trap the AR in an inactive complex by preventing dissociation of heat shock proteins. Previously, it was shown that liganded glucocorticoid receptor binds to the NM by default and that ATP is necessary for subsequent translocation to the nucleus (37). However, in the presence of oligomycin, little AR was seen in the NM fraction; hence, AR movement to the NM appears to be an energy-dependent process. Actin polymerization, previously shown to be essential for androgen-induced AR translocation via its association with filamin (36), is shown here to also be required for AR translocation in response to antiandrogens. The importance of the cytoskeleton was also demonstrated by inhibition of tubulin polymerization. This permits AR translocation to the NM fraction (but not the nucleus) when cells are treated with agonist (MB) or the partial antagonists CPA and OHF, but not the pure antagonist BIC, suggesting that both inhibition by BIC and activation by ligand involve association with tubulin and the cytoskeleton. The 2-DE of the NM and 9 mol/L urea fractions identified a high proportion of structural proteins including actin and myosin.

Our results, together with those of Dotzlaw *et al.* (38), who showed that CPA but not OHF or BIC promoted the recruitment of corepressors to the AR, demonstrate that different therapeutic antiandrogens act via differing mechanisms. We show that OHF and BIC cause reversible AR translocation to the NM, possibly by different processes, whereas CPA may act by nonreversible sequestration of AR in the cytoplasm. This is the first evidence for alternative localization of the AR after treatment with different antiandrogens in prostate cancer cells. It is vital to understand how antiandrogens exert their effects to understand why antiandrogen treatment inevitably fails. One potential mechanism is mutation of the AR itself, which is estimated to occur in 20% to 40% of cases of advanced prostate cancer and increases in incidence in hormone-refractory disease (reviewed

in ref. 39). In some cases, the mutations allow the AR to become activated by adrenal androgens, estrogen, and antiandrogens, providing a mechanism for AR-dependent growth in the absence of gonadal androgens and presence of antiandrogens (13, 40, 41). In around 30% of advanced prostate cancers, AR levels appear to be amplified (39), which may result in AR antagonists acting as weak agonists (42). However, the majority of tumors continue to express normal levels of wild-type AR but still recur on antiandrogen therapy, suggesting that whereas AR signaling is still required for growth, the inhibitory action of the antiandrogen has been circumvented by other means. These could include alterations in levels or activity of proteins involved in localization of the AR in response to antiandrogens or maintaining it in an inactive state. Our studies show that these mechanisms (and thus perhaps the proteins involved) differ for different antiandrogens. This may prove significant for the future treatment of prostate cancer patients with these ligands, possibly providing the basis for a rational sequence of antiandrogens in treatment, thus prolonging the relapse-free period and life expectancy. This has already been established in breast cancer, in which treatment with the antiestrogen faslodex after a patient has relapsed on tamoxifen leads to clinical benefit in around 40% of patients (43). Although treatment with a second antiandrogen after one has failed is not common practice in prostate cancer therapy at present, our study suggests that, for instance, failure of flutamide therapy may not preclude a response to cyproterone acetate. We have also shown that the PC3wtAR cell line is an effective model for investigating antiandrogens, providing new avenues to investigate the mechanism of androgen resistance in prostate cancer.

## ACKNOWLEDGMENTS

We are grateful to Dr. Sigrun Mink for technical expertise and assistance. We also thank AstraZeneca and Schering-Plough for the kind gifts of antiandrogens and Dr. S. Ali, Prof. M. Parker, and members of the Prostate Cancer Research Group Imperial College London, London, United Kingdom for helpful discussion and criticism.

## REFERENCES

1. Crawford ED. Epidemiology of prostate cancer. *Urology* 2003;62:3–12.
2. Dauvois S, White R, Parker MG. The antiestrogen ICI 182780 disrupts estrogen receptor nucleocytoplasmic shuttling. *J Cell Sci* 1993; 106:1377–88.
3. Guiochon-Mantel A, Lescop P, Christin-Maitre S, et al. Nucleocytoplasmic shuttling of the progesterone receptor. *EMBO J* 1991;10: 3851–9.
4. Hache RJ, Tse R, Reich T, Savory JG, Lefebvre YA. Nucleocytoplasmic trafficking of steroid-free glucocorticoid receptor. *J Biol Chem* 1999;274:1432–9.
5. Kempainen JA, Lane MV, Sar M, Wilson EM. Androgen receptor phosphorylation, turnover, nuclear transport and transcriptional activation. *J Biol Chem* 1992;267:968–74.
6. Jenster G, Trapman J, Brinkmann AO. Nuclear import of the human androgen receptor. *Biochem J* 1993;293:761–8.
7. Georget V, Lobaccaro JM, Terouanne B, et al. Trafficking of the androgen receptor in living cells with fused green fluorescent protein-androgen receptor. *Mol Cell Endocrinol* 1997;129:17–26.
8. Waller AS, Sharrard RM, Berthon P, Maitland NJ. AR localisation and turnover in human prostate epithelium treated with the antiandrogen casodex. *J Mol Endocrinol* 2000;24:339–51.

9. Tyagi RK, Lavrovsky Y, Ahn SC, et al. Dynamics of intracellular movement and nucleocytoplasmic recycling of the ligand activated androgen receptor in living cells. *Mol Endocrinol* 2000;14:1162–74.
10. Pratt WB, Toft DO. Regulation of signaling protein function and trafficking by the hsp90/hsp70-based chaperone machinery. *Exp Biol Med (Maywood)* 2003;228:111–33.
11. Warriar N, Page N, Koutsilieris M, Govindan MV. Interaction of antiandrogen-androgen receptor complexes with DNA and transcription activation. *J Steroid Biochem Mol Biol* 1993;46:699–711.
12. Masiello D, Cheng S, Bublely GJ, Lu ML, Balk SP. Bicalutamide functions as an androgen receptor antagonist by assembly of a transcriptionally inactive receptor. *J Biol Chem* 2002;277:26321–6.
13. Veldscholte J, Berrevoets CA, Ris-Stalpers C, et al. The androgen receptor in LNCaP cells contains a mutation in the ligand-binding domain which affects steroid binding characteristics and response to antiandrogens. *J Steroid Biochem Mol Biol* 1992;41:665–9.
14. Peterziel H, Mink S, Schonert A, et al. Rapid signalling by androgen receptor in prostate cancer cells. *Oncogene* 1999;18:6322–9.
15. Ray DW, Davis JRE, A W, Clark AJL. Glucocorticoid receptor structure and function in glucocorticoid-resistant small cell carcinoma cells. *Cancer Res* 1996;56:3276–80.
16. Staufenbiel M, Deppert W. Preparation of nuclear matrices from cultured cells: subfractionation of nuclei in situ. *J Cell Biol* 1984;98:1886–94.
17. Trapman J, Klaasen P, Kuiper GGJM, et al. Cloning, structure and expression of a cDNA encoding the human androgen receptor. *Biochem Biophys Res Commun* 1988;153:241–8.
18. Gamble SC, Odontiadis M, Waxman J, et al. Androgens target prohibitin to regulate proliferation of prostate cancer cells. *Oncogene* 2004;23:2996–3004.
19. Jindal S, Dudani A, Singh B, Harley C, Gupta R. Primary structure of a human mitochondrial protein homologous to the bacterial and plant chaperonins and to the 65-kilodalton mycobacterial antigen. *Mol Cell Biol* 1989;9:2279–83.
20. Tong WM, Cortes U, Wang ZQ. Poly(ADP-ribose) polymerase: a guardian angel protecting the genome and suppressing tumorigenesis. *Biochim Biophys Acta* 2001;1552:27–37.
21. Goldman RD, Gruenbaum Y, Moir RD, Shumaker DK, Spann TP. Nuclear lamins: building blocks of nuclear architecture. *Genes Dev* 2002;16:533–47.
22. MacGillivray RT, Mendez E, Sinha SK, et al. The complete amino acid sequence of human serum transferrin. *Proc Natl Acad Sci USA* 1982;79:2504–8.
23. Vorum H, Liu X, Madsen P, Rasmussen HH, Honore B. Molecular cloning of a cDNA encoding human calumenin, expression in *Escherichia coli* and analysis of its Ca<sup>2+</sup>-binding activity. *Biochim Biophys Acta* 1998;1386:121–31.
24. Kato H, Fukuda T, Parkison C, McPhie P, Cheng SY. Cytosolic thyroid hormone-binding protein is a monomer of pyruvate kinase. *Proc Natl Acad Sci USA* 1989;86:7861–5.
25. Lopez-Fanarraga M, Avila J, Guasch A, Coll M, Zabala JC. Review: postchaperonin tubulin folding cofactors and their role in microtubule dynamics. *J Struct Biol* 2001;135:219–29.
26. Ting J, Lee AS. Human gene encoding the 78,000-dalton glucose-regulated protein and its pseudogene: structure, conservation, and regulation. *DNA* 1988;7:275–86.
27. Shav-Tal Y, Zipori D. PSF and p54(nrb)/NonO: multi-functional nuclear proteins. *FEBS Lett* 2002;531:109–14.
28. Ginisty H, Sicard H, Roger B, Bouvet P. Structure and functions of nucleolin. *J Cell Sci* 1999;112:761–72.
29. Gunning P, Ponte P, Okayama H, et al. Isolation and characterization of full-length cDNA clones for human alpha-, beta-, and gamma-actin mRNAs: skeletal but not cytoplasmic actins have an amino-terminal cysteine that is subsequently removed. *Mol Cell Biol* 1983;3:787–95.
30. Iwasaki T, Murata-Hori M, Ishitobi S, Hosoya H. Diphosphorylated MRLC is required for organization of stress fibers in interphase cells and the contractile ring in dividing cells. *Cell Struct Funct* 2001;26:677–83.
31. Sundstrom BE, Stigbrand TI. Cytokeratins and tissue polypeptide antigen. *Int J Biol Markers* 1994;9:102–8.
32. Helfand BT, Chang L, Goldman RD. Intermediate filaments are dynamic and motile elements of cellular architecture. *J Cell Sci* 2004;117:133–41.
33. Holzmann K, Korosec T, Gerner C, Grimm R, Saueremann G. Identification of human common nuclear-matrix proteins as heterogeneous nuclear ribonucleoproteins H and H' by sequencing and mass spectrometry. *Eur J Biochem* 1997;244:479–86.
34. Ho YS, Crapo JD. Isolation and characterization of complementary DNAs encoding human manganese-containing superoxide dismutase. *FEBS Lett* 1988;229:256–60.
35. Meloun B, Moravek L, Kostka V. Complete amino acid sequence of human serum albumin. *FEBS Lett* 1975;58:134–7.
36. Ozanne DM, Brady ME, Cook S, et al. Androgen receptor nuclear translocation is facilitated by f-actin cross-linking protein filamin. *Mol Endocrinol* 2000;14:1618–26.
37. Tang Y, DeFranco DB. ATP-dependent release of glucocorticoid receptors from the nuclear matrix. *Mol Cell Biol* 1996;16:1989–2001.
38. Dotzlaw H, Moehren U, Mink S, et al. The amino terminus of the human AR is target for corepressor action and antihormone agonism. *Mol Endocrinol* 2002;16:661–73.
39. Taplin ME, Balk SP. Androgen receptor: a key molecule in the progression of prostate cancer to hormone independence. *J Cell Biochem* 2004;91:483–90.
40. Peterziel H, Culig Z, Stober J, et al. Mutant androgen receptors in prostatic tumours distinguish between amino-acid-sequence requirements for transactivation and ligand binding. *Int J Cancer* 1995;63:544–50.
41. Hara T, Miyazaki J, Araki H, et al. Novel mutations of androgen receptor: a possible mechanism of bicalutamide withdrawal syndrome. *Cancer Res* 2003;63:149–53.
42. Chen CD, Welsbie DS, Tran C, et al. Molecular determinants of resistance to antiandrogen therapy. *Nat Med* 2004;10:33–9.
43. Morris C, Wakeling A. Fulvestrant (“Faslodex”): a new treatment option for patients progressing on prior endocrine therapy. *Endocr Relat Cancer* 2002;9:267–76.